Quadruply-labeled serum albumin as a biodegradable nanosensor for simultaneous fluorescence imaging of intracellular pH values, oxygen and temperature

Xiao-ai Zhang[1], Wei Zhang[1], Qi Wang[2], Junli Wang[3], Guodong Ren[3], Xu-dong Wang[1,*]

1. Department of Chemistry, Fudan University, Songhu Road 2005, 200438 Shanghai, China
2. Laboratory of Biophysics, University of Turku, FI-20014 Turku, Finland
3. State Key Laboratory of Genetic Engineering and Department of Biochemistry and Molecular Biology, School of Life Sciences, Fudan University, Shanghai 200438, China

Corresponding Author: wangxudong@fudan.edu.cn

Keywords: simultaneous imaging, multiple sensing, triple sensing, nanosensors, luminescence, intracellular sensing, serum albumin, ratiometric pH sensing, lifetime imaging, oxygen sensing

Abstract: The construction of multiple fluorescent nanosensors for intracellular studies is a challenging task because spectral overlap of indicator probes can lead to cross-talk and mutual interference. This work describes biodegradable nanosensors that can simultaneously measure three intracellular parameters (temperature, pH and oxygen concentration). Bovine serum albumin (BSA) is selected as the scaffold to construct the triple nanosensor by covalent immobilization four fluorophores on BSA. The following luminophores were used: (a) fluorescein as a probe for pH values, (b) a platinum (II) porphyrin complex for oxygen; (c) a europium (III) clathrate complex for temperature, and (d) a rhodamine B as a reference dye. The nanoparticles have a size of 20 nm and show excellent biocompatibility and good brightness. The nanosensors were used for ratiometric imaging of intracellular pH values, oxygen and temperature in HeLa cells. The triple nanosensor responds reversibly and this can be used for real-time tracing of these key parameters. Owing to their biodegradable feature, the use of this kind of triple nanosensor reduce the stress on cellular activities because less nanosensors can be used to gather the total information.

Introduction

Biological processes, including cell proliferation, apoptosis, signaling, and endocytosis, are highly affected and regulated by key physiological parameters, such as intracellular pH, oxygen and temperature. For example, intracellular pH is highly involved in adjusting hydrolase activity and proton-involved reactions [1]. Molecular oxygen is one of the most important food stuff for cells, and its concentration is closely related to energy production [2]. A suitable temperature is required to maintain chemical equilibrium of various endothermic or exothermic processes. All these fundamental parameters are closely related to cell metabolism, and they are strongly interconnected and interacted with each other [3]. A slight change of one parameter leads to a series of syndromes and cellular dysfunctions. This also results in changes in the other two indexes. Abnormal temperature, for instance, may cause inflammation of tissues [4], which is often accompanied by tissue acidosis [5]

and severe hypoxia [6]. Researches have revealed that cancer cells can be characterized by their special microenvironment caused by acidification [7,5], hypoxia [8] and higher temperature [7]. Therefore, simultaneous and accurate measurements of intracellular pH, oxygen partial pressure and temperature play important roles in understanding cellular physiology processes, pharmacology and metabolism, which is extremely useful in diagnosis and therapy of major diseases. Two reports on wearable and ingestible multiple sensors for skin sweat analysis and gastrointestinal health analysis have shown the power of multiple sensing in health care and diagnosis [9,10].

In the past decades, researchers have developed various methods for simultaneously measuring multiple parameters, including microelectrodes [9,10] and optical sensors [11-13]. Compared with the relative large size of microelectrodes, optical sensors have a unique feature that they are capable to measure multiple parameters at the same time, and more importantly, at the same site, while keeping their compact size in the nanodimension. Their size can be easily miniaturized into nanoscale to facilitate intracellular applications. The use of nanosized multiple nanosensors greatly reduces the amount of external materials that has to be introduced into cells. Hence, the interference of foreign materials to cellular activities and metabolism is minimized. More importantly, highly integrated multiple nanosensors provide not only greatly improved spatial resolution, but also the opportunity to study intracellular events at subcellular level.

Driven by continuous innovation in new fluorescent probes, optical nanosensors for a single parameter measurement have been extensively developed, and their numbers are still fast growing [14,15]. Different kinds of single nanosensors for pH and oxygen are available with distinct sensitivity, measurement range and targeting capability [16,17]. Some of them are even commercial-available, such as mitoXpress etc [16]. However, the development of multiple nanosensors is not as simple as expected [18]. The success of multiple planar sensors cannot be easily applied to the development of nanoscale multiple sensors, mainly because of the limited space of material at nanodimension. The integration of multiple probes with different physiochemical properties onto a single nanomaterial will either form aggregates to lose their fluorescence, or cause severe signal cross-talk that significantly complicates signal readout and data interpretation. The physiochemical properties of luminescent probes should not only match that of matrix material, but also fit that of the analyte. Lipophilic probes for oxygen, for example, need to be placed in hydrophobic materials with good gas permeability. However, probes for temperature prefer to be embedded in lipophilic materials without gas permeability to minimize cross-talk to oxygen. Hydrophilic pH probes need to be immobilized on sensor surface to facilitate diffusion of protons. The integration of these distinct features on the same nanosensor has been proved to be challenging [3].Thus, the development of multiple optical sensors at nanodimension is still in its infancy and great efforts need to be devoted to push the area forward.

Few, if any, literatures on simultaneously measuring intracellular multiple parameters have been reported. Zhang's group reported a dual nanosensor for measuring intracellular pH and temperature. A luminescent europium complex and the pH-sensitive fluorescein were covalently labeled on a temperature-sensitive polymer, P(NIPAAM-co-HEMA)-*b*-PVP [19].The formed micelle showed obvious color and fluorescence change when pH varying from 5.0 to 8.0, and temperature from 15 to 45 °C. Another multiple sensor was developed to measure intracellular pH and temperature simultaneously by Qian and coworkers [20]. A pH-sensitive probe was labeled on a temperature-sensitive polymer poly (*N*-isopropylacrylamide) to form spherical nanosensor. The dual nanosensor measured pH in the range of 5-9 and temperature from 25 to 37 °C. In the same year, we designed the first ultra-small ratiometric nanosensor for measuring intracellular pH and oxygen directly in the cytosol

[3]. A Pluronic polymer with unique structure was employed as matrix, which formed a core/shell micelle structure in aqueous solution. The core was hydrophobic that can be used for encapsulating the lipophilic reference dye and the oxygen-sensitive probe. The hydrophilic pH-sensitive indicator was covalently immobilized on the hydrophilic shell. The nanostructure was solidified by silica growth, and resulting nanosensor with the size of only 12 nm. Owing to the unique nanostructure, the nanosensor exhibited excellent sensitivity and good biocompatibility. Other dual nanosensors, including nanosensors for pH and temperature [21], for pH and oxygen [8], for pH and Cu^{2+}, for pH and $O_2^{\bullet-}$ [22], for Fe^{2+} and Cu^{2+} [23], for pH and hydrogen peroxide [24], and for glucose and hydrogen peroxide [25] were also developed. However, unlike film based sensors which are capable of simultaneously measuring three or four parameters [26,27], nanosized sensors for intracellular multiple sensing do not cross the obstacle of measuring more than two parameters at the same time. This is mainly because more than four different kinds of luminophores need to be immobilized on a single particle, while still keeping their luminescence, maintaining good brightness, and retaining their compact size. Signal readout would be complicated by cross-talking, Förster resonance energy transfer (FRET) pair, self-quenching and spectral overlap. In addition, temperature sensing and compensation are mandatory for multiple sensing, because the luminescence of luminophores is influenced by temperature [17]. In addition, intracellular uneven temperature distribution [28,29] leads to measurement inaccuracy.

Herein, we report quadruple-fluorophore-labeled serum albumins as triple nanosensors for simultaneously imaging intracellular pH, oxygen and temperature. The nanosensors exhibit good biocompatibility and are biodegradable, which endows them suitable for intracellular studies without severely interrupting normal cellular activities. The triple nanosensors are constructed using serum albumins as building blocks. Native bovine serum albumins were modified with amino groups to increase the number of amino groups on protein surface. The reactive amino groups on protein surface were then covalently labeled with four fluorophores, which forms the triple nanosensors. Fluorophores were carefully selected to prevent self-quenching, and signal cross-talking. All three parameters were measured in referenced mode, which greatly enhances the precision and accuracy of intracellular measurements. The influences of cellular autofluorescence and system alignment have been greatly suppressed. Results show the nanosensors have good responses to dissolved oxygen, pH and temperature in the physiological range, which is beneficial for intracellular studies. These nanosensors have been proved to be biodegradable, and can be easily taken up by cells via endocytosis. The triple nanosensors can be directly used for sensing and imaging intracellular oxygen, pH and temperature values.

Experimental Section

Materials

Bovine serum albumin (BSA), MOPs sodium salt (NaMOPs), Glucose oxidase, Hank's balanced salt solution, minimum essential medium eagle, penicillin-streptomycin solution, L-glutamine solution and Minimum Essential Medium Eagle (MEM) nonessential amino acid solution (100X) were bought from Sigma-Aldrich (www.sigmaaldrich.com). Fluorescein isothiocyanate (FITC, mixture of 5- and 6- isomers) and rhodamine B isothiocyanate (RBITC) were purchased from Heowns (www.heowns.com). Pt (II) meso-tetra (4-carboxyphenyl) porphine (PtTCPP) was bought from J&K Chemical (www.jkchemical.com). The Eu clathrate (Na_2 ($EuC_{34}H_{33}O_{14}N_{10}$)) was received as a gift from Dr. Qi Wang in University of Turku (Finland). Ethylenediamine dihydrochloride (EDA), *N*-hydroxysuccinimide (NHS), 1-(3-dimethylaminopropyl)-3-ethylcarbodimide hydrochloride (EDC), glucose, fluorescamine and Coomassie blue were obtained from Tokyo Chemical Industry

(www.tcichemicals.com). Sephadex G-50 and nigericin were bought from Yuanyebio Co., Ltd (www.shyuanye.com, Shanghai, China). Fetal bovine serum was purchased from Tianhang Biotechnology Co., Ltd. (www.hzsjq.com, Hangzhou, China). Phosphate buffered saline (PBS) with pH in the range of 7.2-7.4 was bought from BBI Life Sciences (www.bbi-lifesciences.com, Shanghai, China). Trypsin was purchased from Thermo-Fisher under the brand Gibco (www.thermofisher.com). CCK-8 Cell Counting Kit was purchased from Dojindo (www.dojindo.cn). Cell imaging and viability tests were performed in living HeLa cells. All chemicals were used as received without further purification, and all solutions were prepared using deionized distilled water.

Preparation of cationic BSA (cBSA)

BSA has limited free amino groups on its surface. In order to create more reactive amino groups to facilitate fluorescent probes labeling, BSA was modified using EDA to give cationic BSA, which is denoted as cBSA later on. A degassed EDA solution (2.5 mol·L^{-1}) was prepared by dissolving EDA (4.99 g, 37.5 mmol) in 15 mL of deionized distilled water, followed by adjusting solution pH to 4.75 and degassing under vacuum for 30 min. Then BSA (150 mg, 2.26 μmol) was dissolved in the degassed EDA solution under stirring. The modification was initiated by adding EDC (766.8 mg, 4 mmol) in the above solution and the mixture was stirred for 75 min. Finally, acetate buffer (1.0 mL, 4.0 mol·L^{-1}, pH 4.75) was added to quench the reaction. The cBSA was isolated using an ultrafiltration tube (type Vivaspin 20) with centrifugal force at 6000 g for 40 min, followed by washing steps using deionized distilled water. The washing and centrifugation processes were repeated 6 times to remove unreacted chemicals, and the cBSA was diluted to 10 mL in deionized distilled water and stored at 4 °C.

Synthesis of the multiple nanosensor

The cBSA was further labeled with four different fluorophores to construct the triple nanosensor for oxygen, pH and temperature. The labeling made use of amino groups on cBSA to react with NHS-activated dyes and dyes with reactive isothiocyanate groups. The oxygen-sensitive probe PtTCPP and the temperature-sensitive europium complex possess carboxyl groups in their chemical structures, which was activated via the EDC-NHS approach. The NHS-activated dyes can be easily labeled on cBSA surface by forming covalent bonds. Typically, PtTCPP (20 μL, 3.75 mmol·L^{-1}, 75 nmol) and the Eu clathrate (15 μL, 2.22 mmol·L^{-1}, 33.3 nmol) were activated by reacting with EDC and NHS for 1.0 h and 4.0 h respectively. The NHS-activated dyes were added into a mixture containing cBSA solution (250 μL, 12 mg·mL^{-1}), phosphate buffer (250 μL, pH 8.0), and RBITC solution (20 μL, 10 mmol·L^{-1} in DMF, 200 nmol). The mixture was protected from light, and put on an IKA trayster rotator for 2.0 h. Then FITC solution (5 μL, 1.0 mmol·L^{-1} in DMF, 5.0 nmol) was added, and the solution was further rotated for 24.0 h. Afterwards, the solution was centrifuged at 10 000 g for 10 min to remove large aggregates. The solution was purified using a Sephadex G-50 column to remove unbounded dyes and unreacted chemicals. The purified solution was concentrated in vacuum to a concentration of 650 μg·mL^{-1}. The nanosensor suspension was placed in dark and stored at 4.0 °C before use.

Biodegradation of the nanosensor

The sodium dodecyl sulfate polyacrylamide gel electrophoresis (SDS-PAGE) was used to analyze the biodegradation of BSA, cBSA and the triple nanosensor. In brief, 1 μL of trypsin (0.1 mg·mL^{-1}) was added to 9.0 μL of samples and incubated at 37 °C for indicated time periods. To deactivate trypsin protease, 3 μL of 5x SDS loading buffer was added to the mixture

and boiled for 9 minutes. All samples were then analyzed on SDS-PAGE and stained with Coomassie blue. The concentration of BSA and cBSA were both at 500 $\mu g \cdot mL^{-1}$, and the solution of the triple nanosensor was also diluted to about 500 $\mu g \cdot mL^{-1}$.

Cell culture and fluorescent imaging

HeLa cells were purchased from the Cell Bank of Chinese Academy of Sciences (Shanghai, China), and were cultivated at 37 °C in an atmosphere containing 5% CO_2. The culture medium contained 87% Minimum Essential Medium Eagle (MEM, Sigma Aldrich), 10% fetal bovine serum (FBS), 1% MEM nonessential amino acid solution (100X), 1% Penicillin-Streptomycin and 1% L-Glutamine solution. For intracellular imaging, HeLa cells were incubated with nanosensors suspension (typically 160 $\mu g \cdot mL^{-1}$) for 4.0 h, and then washed using Hank's balanced salt solution to remove free nanosensors in the culture media. These cells were then imaged using the microscope.

For intracellular measurement of temperature, HeLa cells loaded with nanosensors were firstly equilibrated for 10 min at temperatures from 30 °C to 40 °C using a circulating water bath (Huber CC-6, Germany). Then cells were imaged on the fluorescence microscopy with filter set for Europium complex. Lifetime data was measured using the FLS1000 fluorometer (Edinburgh, UK). For intracellular pH imaging, HeLa cells loaded with nanosensors were incubated in a high K^+ buffer (130 $mmol \cdot L^{-1}$ KCl, 10 $mmol \cdot L^{-1}$ NaCl, 1 $mmol \cdot L^{-1}$ $MgSO_4$, 10 $mmol \cdot L^{-1}$ NaMOPs) at various pH of 4, 6 and 9, together with 10 $\mu g \cdot mL^{-1}$ of nigericin for 15 min to adjust pH. Then the cells were imaged on the fluorescence microscopy with filter sets for FITC and Rhodamine. For intracellular oxygen response study, 20 μL of glucose and 20 μL of glucose oxidase were added to HeLa culture medium to consume oxygen, and the luminescence intensity change of PtTCPP were recorded using the fluorescence microscope.

Cell viability test

HeLa cells with a density of 1×10^4 cells/well were seeded on a 96-well plate, and incubated overnight in MEM media. Then, the triple nanosensors were added at various concentration from 0 to 325 $\mu g \cdot mL^{-1}$. After another 24 h incubation, the cytotoxicity of nanosensor was evaluated using CCK-8 Cell Counting Kit. A multitier plate reader (Biotek Synergy H1) was used for measuring absorbance at 450 nm (absorbance of living cells) and 650 nm (absorbance of background) for reference.

Instrumentation and Characterization

Zeta potential measurements were performed on a Malvern Zetasizer Nano-ZS at 25 °C. The transmission electron microscopy (TEM) image of the nanosensor was obtained using a Tecnai G2 F20 S-Twin TEM. The atom force microscopic (AFM) measurement was performed on a Bruker Edge in the tapping mode at room temperature. All fluorescence spectra were recorded on a fluorescence spectrophotometer (Hitachi F-7000, Japan). Lifetime measurements were performed on a photoluminescence spectrometer (Edinburgh FLS 1000, United Kingdom). Synthetic gas at a given oxygen concentration was obtained by mixing different volumes of nitrogen and oxygen. The gas flow rates were controlled by two gas-flow meters from Vögtlin (Switzerland). Temperature was precisely adjusted and controlled using a circulating water bath (Huber CC-6, Germany). Intracellular images of the nanosensors were acquired using an inverted fluorescence microscope (Leica DMi8, Germany). The information of filter set for cell imaging was listed in Table S1 in the supplemental material.

Results and Discussion

Serum albumin is essential to maintain the oncotic pressure needed for proper distribution of body fluids between blood vessels and body tissues. Native bovine serum albumin possesses around 60 accessible primary amino groups, which can be directly explored for dye labeling [30]. In order to enhance the brightness of dye-labeled BSA, Weil and coworkers developed modified BSA species using EDA, and created cationic albumin protein that possesses as many as 147 primary amino groups on its surface [30]. During the modification, the molar ratio of EDA to protein was controlled at more than 15 000:1 to prevent protein cross-linking. The new cBSA has been proved to be one of the most efficient and stable transfection agents for DNA and drug delivery [31]. We envisioned that the increased number of primary amino groups on albumin protein surface could be explored for labeling different fluorescent dyes, and create multiple sensors for intracellular study.

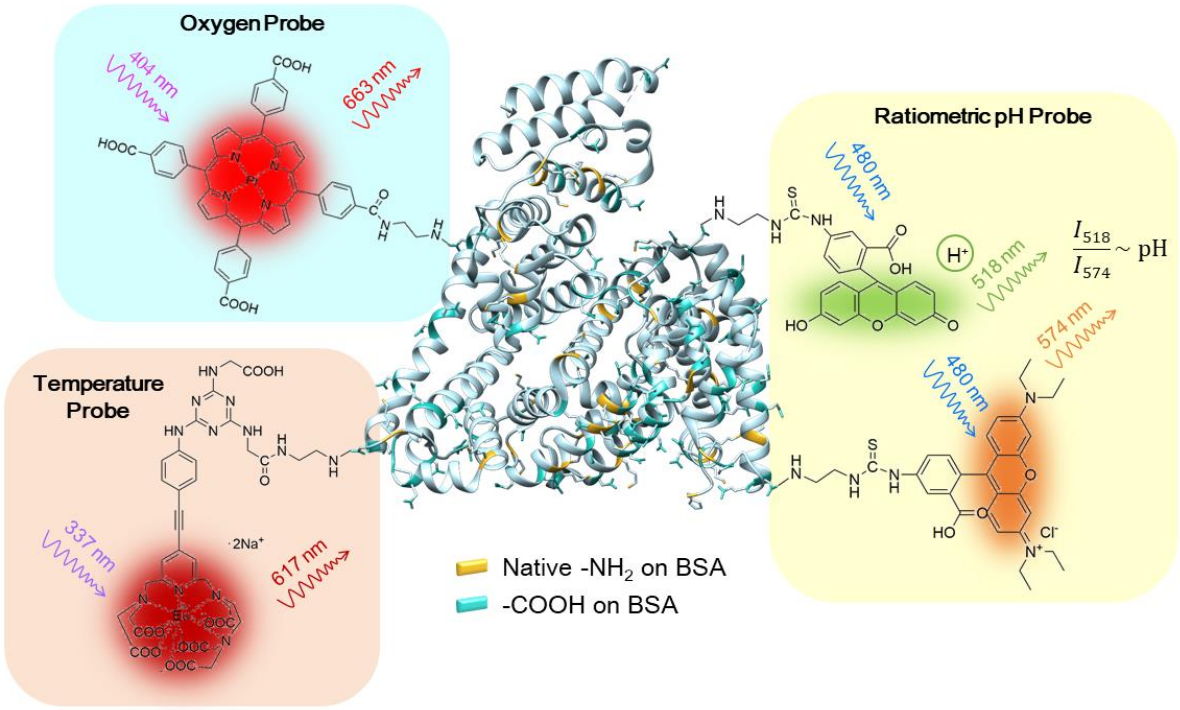

Scheme 1. Scheme of synthetic steps for the triple nanosensor. PtTCPP and Eu clathrate were activated via the EDC-NHS approach to form active NHS-ester, and all four dyes were labeled on the cationic BSA surface via a one-pot reaction

Since modified cBSA has a hydrodynamic radii at 7.1 nm in aqueous solution [30], the selection of fluorescent probes becomes essential to prevent signal cross-talking, and maintain good brightness at the same time. First, all dyes need to have good stability in aqueous solution to prevent protein precipitation after labeling. Second, they should exhibit high brightness in fluorescence imaging at microscopic level. Third, the indicator dyes should have distinct excitation and emission spectra so that no signal cross-talking happens. A careful screening of suitable probes for pH, oxygen and temperature resulted in the following dyes (as shown in Scheme 1): FITC was selected as the pH-sensitive probe since its *p*Ka at 6.5 matches well with the physiological pH range. The water-soluble platinum porphyrin PtTCPP was used as an oxygen indicator, because of its long lifetime and high sensitivity in the range of 0-10.0 $mg \cdot L^{-1}$ dissolved oxygen [32]. Its sharp emission peak at 663 nm separates well with other fluorophores. A stable and water-soluble europium clathrate with extremely sharp emission peak at

617 nm and long decay time (in millisecond range, Fig. S1) was chosen as the temperature probe. The long phosphorescent lifetime of PtTCPP and Eu clathrate enables lifetime based measurement which offers high accuracy and low interference from external source, since phosphorescent lifetime is an intrinsic physical property of luminophores, and is independent with microenvironment and other external factors [33,17]. The pH indicator possesses short lifetime in nanosecond range, and is difficult to be measured precisely. Thus, a reference dye, Rhodamine B, emitting at 574 nm was selected to form a ratiometric sensor for pH measurement. The introduction of the reference dye enables ratiometric readout of the signal, which avoids the influence of autofluorescence and fluctuation of light source, system alignment and local probe concentration and distribution [8,4]. All the fluorescent probes were chosen in such a way that there is no spectra or lifetime overlap for pH, oxygen, and temperature measurement, which not only prevents signal cross-talking, but also makes signal readout and analysis simpler (as shown in Fig. S2).

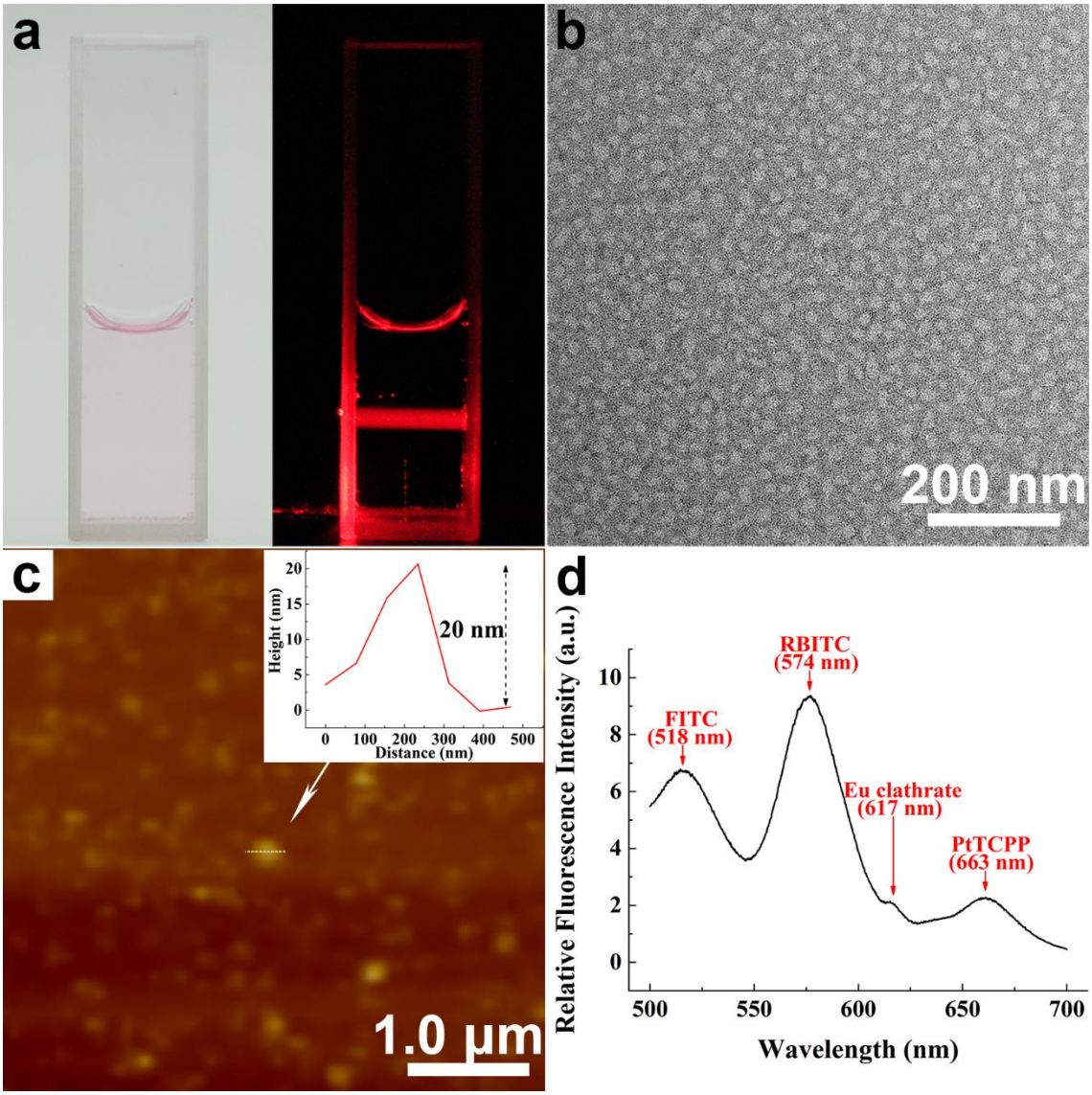

Fig. 1 (a) Suspension of nanosensors in water (left) and the Tyndall effect (right); (b) TEM image of the nanosensors, showing their average diameter is ~ 20 nm; (c) AFM image of the nanosensors on the silicon wafer, and the insert shows the diameter of the nanosensor; (d) Emission spectra of the nanosensor excited at 400 nm. Four luminescence peaks at 518 nm, 574 nm, 617 nm and 663 nm confirm successful labeling of four fluorophores on cBSA

In order to increase the number of surface reactive groups on native BSA, EDA was used to convert the surface free carboxyl groups into amino groups. The cationic BSA showed an increased number of amino groups as quantified using fluorescamine method (Fig. S3). Zeta potential measurements of BSA and cBSA revealed that surface charge was changed from -12.8 mV of BSA to positive 12.4 mV after EDA modification, indicating the success of converting surface carboxyl groups into positively-charged amino groups. The labeling of three indicator dyes and the reference dye on cBSA was straightforward. PtTCPP and the Eu clathrate bearing carboxyl groups were firstly activated via EDC-NHS approach to form NHS ester, which were then reacted with amino groups on the surface of cBSA to form stable covalent bonds. The pH-sensitive probe FITC and the reference dye RBITC have reactive isothiocyanate groups in their chemical structures, which react directly with amino groups to form stable chemical bonds (Scheme 1). All four dyes were then labeled on cBSA via a one-pot reaction. After labeling, the solution was firstly centrifuged to remove large aggregates, and then unlabeled dyes and unreacted chemicals were removed using size exclusion chromatography. The nanosensor suspension is a clear and transparent pink solution (Fig. 1a, left), which proves the good dispersity of nanosensor in water. When a red laser beam was shined onto the solution, the typical Tyndall effect was observed (Fig. 1a, right), which confirms the formation of colloidal nanosensors. TEM image with inverse protein staining shows that the nanosensor has a diameter of ~20 nm (Fig. 1b), which is also confirmed by AFM data (Fig. 1c). The relative large size of nanosensors may be attributed to the cross-linking of BSA during cationic modification.

The nanosensors were then tested for their responses to temperature, pH and oxygen. When the nanosensor suspension was excited at 400 nm, it emitted at three major wavelength peaked at 518 nm, 574 nm, and 663 nm (as shown in Fig. 1d), corresponding to the emissions of Fluorescein, Rhodamine and PtTCPP. Since the Eu clathrate is not efficiently excited at this wavelength, its emission peak at 617 nm is not very strong (a small shoulder peak in Fig. 1d). However, once excited at shorter wavelength (such as 337 nm), the emission of Eu clathrate becomes much stronger (Fig. S4). Simultaneous observation of four emission peaks confirms the successful labeling of four dyes on cBSA.

Since luminescence of any fluorophores are somehow influenced by temperature [17], the triple nanosensor was firstly subjected for temperature measurement. Some researchers have revealed the heterogeneous distribution of heat inside cells, which provides vital information of intracellular activity and functionality [28,29]. The Eu-clathrate possesses long luminescent lifetime in millisecond range, which enables the sensing of temperature based on self-referenced lifetime measurement. As shown in Fig. 2a, once excited at 337 nm, the luminescence lifetime of the Eu-clathrate decreases linearly when temperature rising from 30 to 60 °C. Fig. S5 and S6 in the supplemental material shows the influence of pH and oxygen on the temperature measurement. It is clear that the emission of Eu-clathrate is not influenced by either pH or oxygen variation.

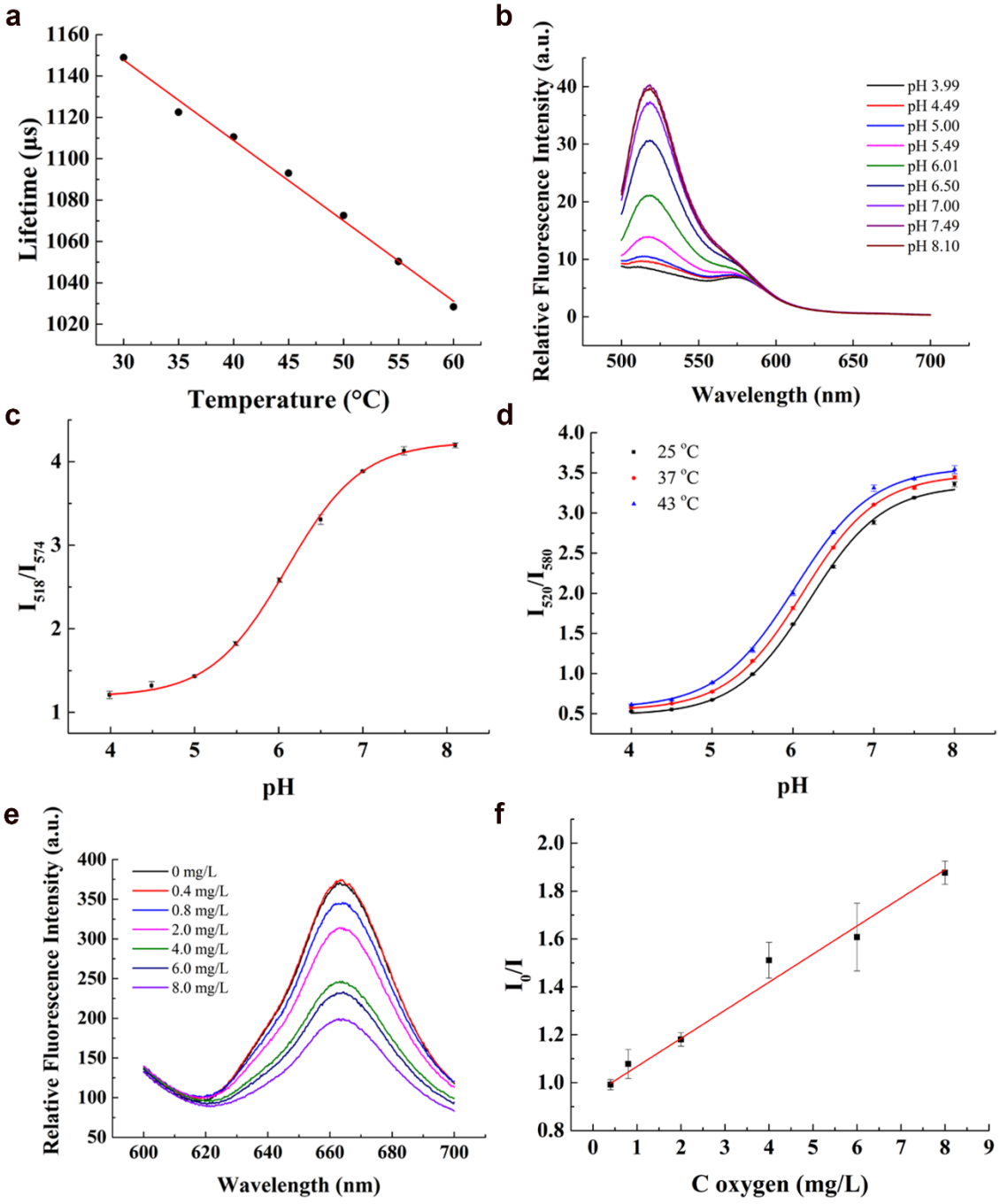

Fig. 2 Calibration plot of Eu clathrate lifetime to temperature (a), emission spectra (b, e) and calibration plots (c, f) of the nanosensor at different pH (b, c) and different concentration of oxygen (e, f), and pH calibration plots at different temperature (d); The nanosensors were excited at 337 nm, 480 nm and 404 nm for temperature, pH and oxygen sensing, respectively

The response of the nanosensor to pH was studied in pH buffer solutions with known pH in the range of 4.0-8.0. As shown in Fig. 2b, once excited at 480 nm, the emission of FITC peaked at 518 nm increased gradually with increasing pH. In contrast, the rhodamine emission at 574 nm only shows slight changes. The reference dye Rhodamine B does not have pH response in

the tested pH range (Fig. S7), the change in fluorescence intensity is mainly due to the spectra overlap of FITC and Rhodamine B or the possible FRET. The intensity ratio at 518 nm and 574 nm correlated well with the solution pH as shown in Fig. 2c. This ratiometric readout can significantly cancel out major influences of light source and sensor uneven distribution. The sensor exhibits high measurement precision as shown in Fig. 2c with small error bars. The *p*Ka of the nanosensor is 6.1, which matches well with physiological pH range. The most sensitive pH range is 5.0-7.5, which is suitable for intracellular study as it covers the most useful range of intracellular pH. In order to compensate the influence of temperature variation on pH sensing, the calibration plots of the nanosensor at different temperatures were studied in details. As shown in Fig. 2d, the variation of temperature presents significant influences on both the *p*Ka and calibration plots for pH sensing. By applying calibration plots at different temperature, pH are measured ratiometrically with the compensation of the influences of temperature. In addition, the influence of oxygen concentration on the pH response of nanosensors was studied. The result shown in Fig. S8 in the supplemental material suggests that the variation of oxygen concentration has ignorable influence on the pH measurement, which proves that the nanosensors do not have cross-sensitivity to the other analyte.

Subsequently, the response of the nanosensor to oxygen was studied. As shown in Fig. 2e, when excited at 404 nm, the luminescence of PtTCPP at 663 nm was quenched efficiently by molecular oxygen. There is a relationship between I_0/I and O_2 concentration, which can be fitted according to the Stern-Volmer equation (Fig. 2f). There is a nearly linear relationship between oxygen concentration and the intensity ratio in the range of 0.4 to 8.0 $mg \cdot L^{-1}$ dissolved oxygen. More importantly, the oxygen-sensitive probe PtTCPP has a long lifetime in microsecond range (52 μs in oxygen-free solution) [34], and the oxygen concentration can be measured via the self-referenced lifetime measurement without the need of a reference dye. Cross-sensitivity test shown in Fig. S9 in the supplemental material reveals that the variation of pH does not influence oxygen sensing. However, similar to pH sensing, the variation of temperature influences oxygen sensing, and its effects can be compensated by applying calibration plots at different temperatures. All these results prove that the three parameters can be measured accurately and separately without worrying about signal cross-talk.

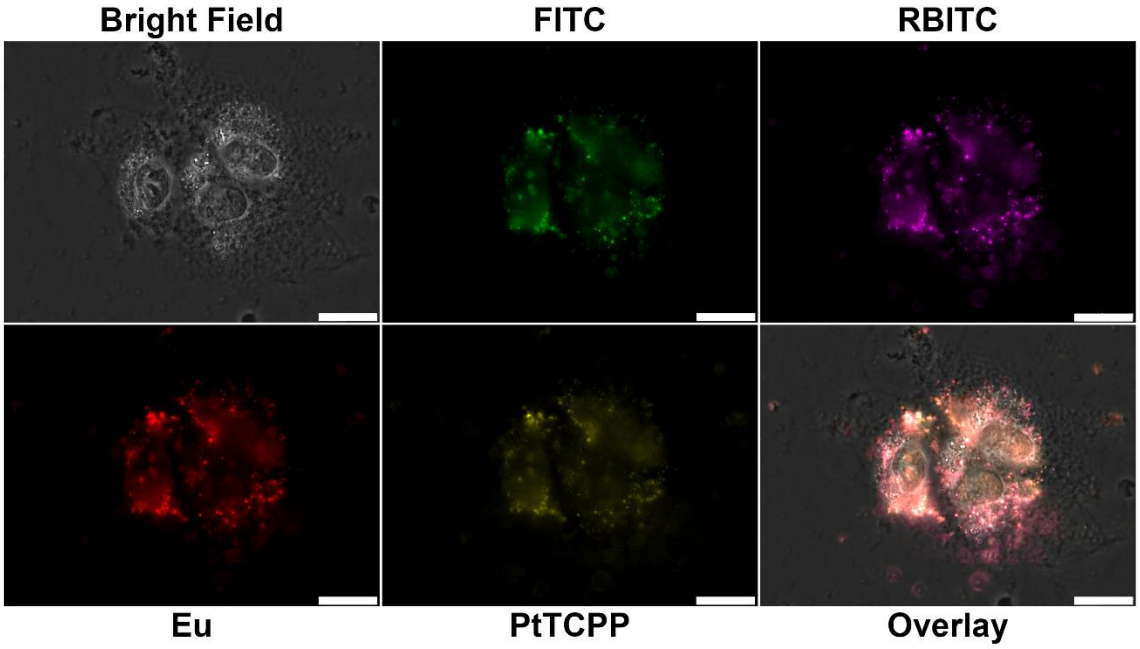

Fig. 3 Bright field and fluorescence microscopic images of HeLa cells incubated with nanosensors; The images are represented in pseudo color: green color for the fluorescence of FITC, magenta for RBITC, red for the Eu clathrate and yellow for PtTCPP; The overlay image shows all luminescence from four dyes located exactly at the same site, indicating successfully labeling of four dyes on the same BSA protein; Scale bar: 20 μm

Before applying the triple nanosensor for intracellular study, their biocompatibility was studied based on cell viability test using CCK-8. The nanosensors were incubated with HeLa cells for 24 hours. After removing free suspended nanosensors in cultivating media, the solution of CCK-8 cell viability test kit was added, and its characteristic absorption at 450 nm was measured to calculate the viability of cells after incubating with nanosensors. As shown in Fig. S10, there is no significant decrease in cell viability, even when the concentration of nanosensors reaches up to 195 $\mu g \cdot mL^{-1}$. When the nanosensor concentration increases to 260 $\mu g \cdot mL^{-1}$, the cell viability remains at approximately 80%, which proves the low cytotoxicity and good biocompatibility of the nanosensor.

The nanosensors were further tested for their biodegradable capability. Trypsin protease was chosen to digest the nanosensors. The digested samples were analyzed using SDS-PAGE and stained with Coomassie blue. As shown in Fig. S11, before adding trypsin, BSA, cBSA and the triple nanosensor all present obvious bands at around 60 kDa, indicating the intact protein before digestion. After adding concentrated trypsin protease, cBSA and the triple nanosensor are hydrolyzed quickly, even at the first ten minutes. BSA shows relatively slow hydrolysis at the same condition, and the reason for the accelerated hydrolysis of cBSA and the triple nanosensor is unknown.

Owing to their good biocompatibility and biodegradability, the nanosensor was finally subjected to measure temperature, pH and oxygen inside HeLa cells. After incubating the nanosensors with HeLa cells, free nanosensors suspended in the culture media were washed for several times, and cells were imaged on the fluorescence microscope. However, due to the strong adsorption of serum to the culture dish, free nanosensors cannot be completely removed by repeated washing as shown in Fig. 3 and Fig. 4. As shown in Fig. 3, the nanosensors were efficiently taken up by HeLa cells. The fluorescence images of each dye were recorded using the corresponding filter set and displayed in Fig. 3 with pseudo color. The green channel represents the fluorescence of FITC, magenta for RBITC, red for the Eu clathrate, and yellow for PtTCPP. From the overlay image, it is clear that all images of four dyes overlapped very well with each other, further proving that all four dyes were successfully labeled on the same cBSA protein. The nanosensors were taken up by HeLa cells via endocytosis. The small size of 20 nm and cationic-charged surface promote the interaction between nanosensors and membranes of HeLa cells [35]. Because of their small size, these sensors are very useful tools to study intracellular activities at the very same site, and with high spatial resolution.

At last, the nanosensors were challenged for their real-time responses to variations of temperature, intracellular pH and oxygen concentration within HeLa cells. The intracellular temperature was adjusted using a circulation bath with precise temperature control. The microscopic images and lifetime of HeLa cells with internalized nanosensors at different temperatures are shown in Fig. 4a, b. It is obvious that the luminescence intensity of Eu-clathrate decreases at elevated temperature. The long luminescent lifetime and good brightness of the dye inside cells enable measuring intracellular temperature based on lifetime measurement (Fig. 4b).

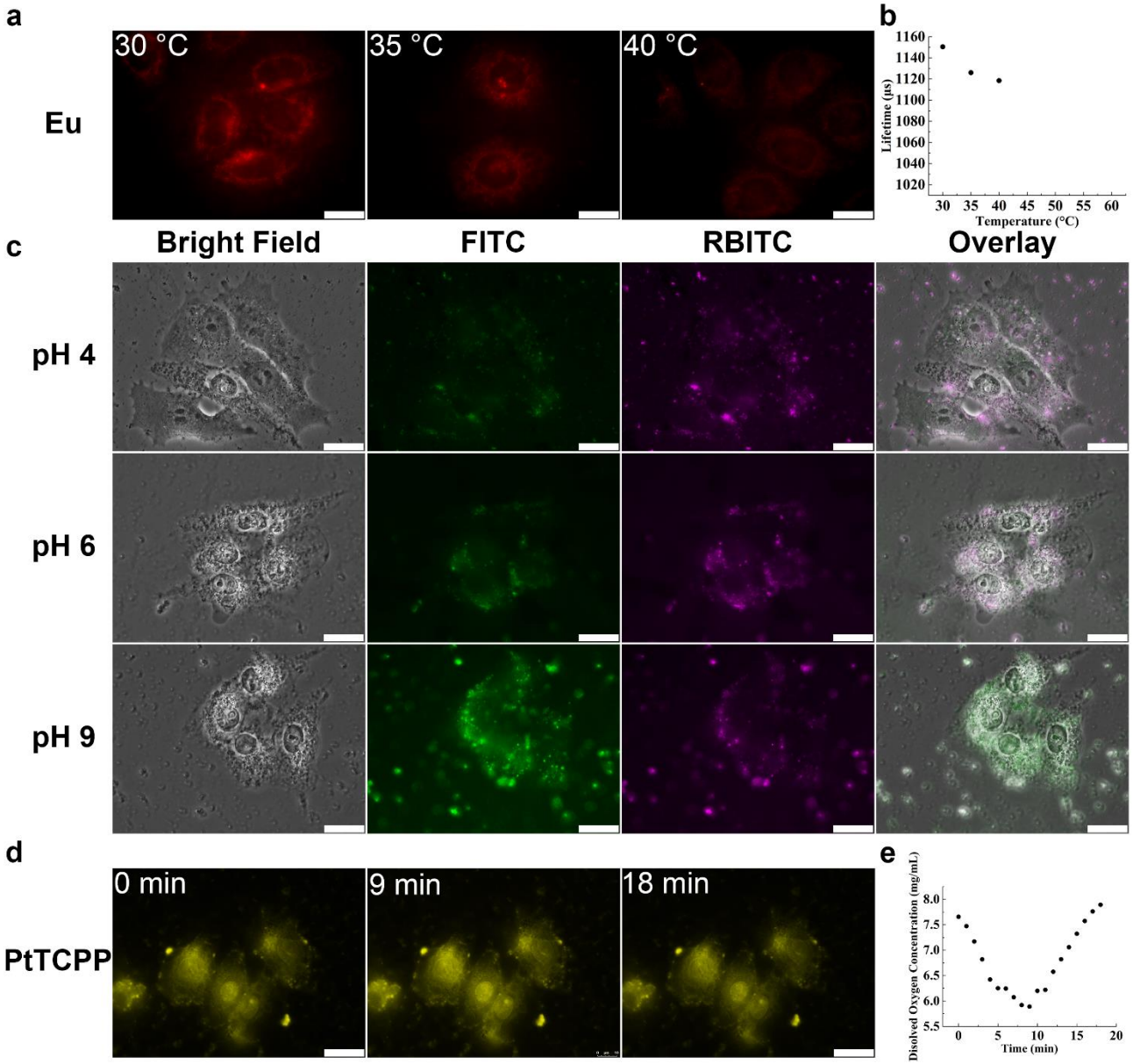

Fig. 4 Intracellular responses of the nanosensors in HeLa cells to temperature (a), pH (c), and dissolved oxygen concentration (d) variation; the lifetime of the Eu clathrate in nanosensors internalized HeLa cells at different temperature was measured by Edinburgh FLS 1000 (b); intracellular oxygen concentration were analyzed using free-software Image-J (e); These images are represented in pseudo color: green for FITC, magenta for RBITC, red for the Eu clathrate and yellow for PtTCPP; Scale bar: 20 μm

Sensing intracellular pH variation was conducted by manipulating intracellular pH values using nigericin and potassium rich buffers at different pH. As shown in Fig. 4c, the fluorescence of FITC (the green channel) enhanced with increasing pH, and that of RBITC remained almost the same. Their luminescence ratio can be explored for measuring intracellular pH. Due

to the different bandpass width and excitation light source between fluorescence spectrophotometer and fluorescence microscope, the calibration plot of the nanosensors at different pH was measured again on the fluorescence microscope. As shown in Fig. S12, the fluorescence intensity ratio of FITC and RBITC shows similar relationship to that measured by the fluorescence spectrophotometer.

The response of the nanosensors to oxygen was also studied intracellularly. A hypoxia extracellular environment was created by consuming dissolved oxygen in the media using glucose and glucose oxidase. As shown in Fig. 4d, at the first 10 min, when dissolved oxygen was consumed, the luminescence intensity of PtTCPP increased overtime. After 10 min, glucose in the media was consumed completely, and molecular oxygen in the air was dissolved in the media again, so the luminescence intensity decreased again. The measurement of dissolved oxygen concentration (Fig. 4e) clearly shows its concentration firstly decreased below 6.0 $mg \cdot L^{-1}$, and then completely recovered back to around 8.0 $mg \cdot L^{-1}$. All these results prove that the nanosensors simultaneously and reversibly measure intracellular temperature, pH and oxygen concentration variation in real time.

Conclusion

In summary, we have developed a good biocompatible and biodegradable multiple nanosensor based on serum albumin protein. By modifying the serum albumin protein with more amino groups, four different fluorophores are successfully labeled on one protein to construct a triple nanosensor for measuring intracellular pH, oxygen and temperature simultaneously. Because of the careful selection of fluorophores, there is no signal cross-talking during the three parameters sensing, which significantly simplifies signal analysis and data interpretation. The triple nanosensor shows good sensitivity and suitable measurement range, which matches well with physiological intracellular values. More importantly, the triple nanosensor exhibits good biocompatibility and is biodegradable, which endows it as an ideal candidate for intracellular sensing and imaging. The nanosensors are finally incubated with HeLa cells, and they can be taken up by HeLa cells via endocytosis. The nanosensors inside HeLa cells show obvious responses to temperature, pH and oxygen change, respectively. Owing to the good biocompatibility, sensitivity, and brightness, and the biodegradable property, this triple nanosensor will be a useful tool to study intracellular events at high spatial resolution. The only limitation of the triple nanosensor for intracellular studies is the requirement of UV excitation for temperature sensing, and the biomatter will create strong autofluorescence to interfere temperature measurement. This imperfection can be easily solved by either phosphorescent lifetime imaging or synthesizing long-wavelength excitable dyes.

Supplemental Material

The filter set used for imaging four dyes inside HeLa cells; Lifetime measurement of the Eu clathrate aqueous solution; Absorption and emission spectra of dyes; Quantification of amino groups of BSA and cBSA; Emission spectra excited at 337 nm at different temperature; The emission spectra of the Eu clathrate at different pH; The influence of oxygen on the emission spectra of the Eu clathrate; The emission spectra of Rhodamine B at different pH; The influence of oxygen on the pH response of the triple nanosensor; The emission spectra of PtTCPP at different pH; Cell viability of HeLa cells co-cultured with nanosensors using CCK-8; Coomassie blue stained SDS-PAGE of BSA, cBSA and the triple nanosensor; The calibration plot of the nanosensor at different pH measured by fluorescent microscope.

Acknowledgements

This work was financially supported by the National Natural Science Foundation of China (21775029), the National Key R&D Program of China (2017YFC0906800), the Recruitment Program of Global Experts (1000 Talent program) in China, and the Program for Professor of Special Appointment (Eastern Scholar) at Shanghai Institutions of Higher Learning (No. TP2014004), which are greatly acknowledged. We thank Anqi Hu from Fudan University for the assistance of AFM measurement.

Compliance with ethical standards

The author(s) declare that they have no competing interests.

References

1. Swietach P, Vaughan-Jones RD, Harris AL, Hulikova A (2014) The chemistry, physiology and pathology of pH in cancer. Philos Trans R Soc, B 369 (1638):20130099. doi:10.1098/rstb.2013.0099
2. Zou X, Pan T, Jiang J, Li G, Song C, Sun R, Yang Z, Sun D, Hou C, Chen M, Tian Y (2017) Poly(ε -caprolactone)-containing graft copolymers for ratiometric extracellular oxygen sensing. Sens Actuator, B 248:108-118. doi:10.1016/j.snb.2017.03.126
3. Wang XD, Stolwijk JA, Lang T, Sperber M, Meier RJ, Wegener J, Wolfbeis OS (2012) Ultra-small, highly stable, and sensitive dual nanosensors for imaging intracellular oxygen and pH in cytosol. J Am Chem Soc 134 (41):17011-17014. doi:10.1021/ja308830e
4. Chen J, Zhang C, Lv K, Wang H, Zhang P, Yi P, Jiang J (2017) A silica nanoparticle-based dual-responsive ratiometric probe for visualizing hypochlorite and temperature with distinct fluorescence signals. Sens Actuator, B 251:533-541. doi:10.1016/j.snb.2017.05.072
5. Hou J-T, Ren WX, Li K, Seo J, Sharma A, Yu X-Q, Kim JS (2017) Fluorescent bioimaging of pH: from design to applications. Chem Sov Rev 46 (8):2076-2090. doi:10.1039/C6CS00719H
6. Eltzschig HK, Carmeliet P (2011) Hypoxia and Inflammation. N Engl J Med 364 (7):656-665. doi:10.1056/NEJMra0910283
7. Liu H, Maruyama H, Masuda T, Honda A, Arai F (2014) Multi-fluorescent micro-sensor for accurate measurement of pH and temperature variations in micro-environments. Sens Actuator, B 203:54-62. doi:10.1016/j.snb.2014.06.079
8. Xu W, Lu S, Xu M, Jiang Y, Wang Y, Chen X (2016) Simultaneous imaging of intracellular pH and O2using functionalized semiconducting polymer dots. J Mater Chem B 4 (2):292-298. doi:10.1039/c5tb02071a
9. Gao W, Emaminejad S, Nyein HYY, Challa S, Chen K, Peck A, Fahad HM, Ota H, Shiraki H, Kiriya D, Lien D-H, Brooks GA, Davis RW, Javey A (2016) Fully integrated wearable sensor arrays for multiplexed in situ perspiration analysis. Nature 529 (7587):509-514. doi:10.1038/nature16521
10. Mimee M, Nadeau P, Hayward A, Carim S, Flanagan S, Jerger L, Collins J, McDonnell S, Swartwout R, Citorik RJ, Bulović V, Langer R, Traverso G, Chandrakasan AP, Lu TK (2018) An ingestible bacterial-electronic system to monitor gastrointestinal health. Science 360 (6391):915-918. doi:10.1126/science.aas9315
11. Miller WW, Yafuso M, Yan CF, Hui HK, Arick S (1987) Performance of an in-vivo, continuous blood-gas monitor with disposable probe. Clin Chem 33 (9):1538-1542
12. Kocincova AS, Borisov SM, Krause C, Wolfbeis OS (2007) Fiber-Optic Microsensors for Simultaneous Sensing of Oxygen and pH, and of Oxygen and Temperature. Anal Chem 79 (22):8486-8493. doi:10.1021/ac070514h
13. Stich MIJ, Fischer LH, Wolfbeis OS (2010) Multiple fluorescent chemical sensing and imaging. Chem Sov Rev 39 (8):3102-3114. doi:10.1039/B909635N
14. Wolfbeis OS (2015) An overview of nanoparticles commonly used in fluorescent bioimaging. Chem Sov Rev 44 (14):4743-4768. doi:10.1039/C4CS00392F
15. Du X, Yang L, Hu W, Wang R, Zhai J, Xie X (2018) A Plasticizer-Free Miniaturized Optical Ion Sensing Platform with Ionophores and Silicon-Based Particles. Anal Chem 90 (9):5818-5824. doi:10.1021/acs.analchem.8b00360

16. Papkovsky DB, Dmitriev RI (2013) Biological detection by optical oxygen sensing. Chem Sov Rev 42 (22):8700-8732. doi:10.1039/C3CS60131E
17. Wang XD, Wolfbeis OS, Meier RJ (2013) Luminescent probes and sensors for temperature. Chem Soc Rev 42 (19):7834-7869. doi:10.1039/c3cs60102a
18. Wolfbeis OS (2013) Probes, sensors, and labels: why is real progress slow? Angew Chem Int Ed Engl 52 (38):9864-9865. doi:10.1002/anie.201305915
19. Li Y-Y, Cheng H, Zhu J-L, Yuan L, Dai Y, Cheng S-X, Zhang X-Z, Zhuo R-X (2009) Temperature- and pH-Sensitive Multicolored Micellar Complexes. Adv Mater 21 (23):2402-2406. doi:doi:10.1002/adma.200803770
20. Yin L, He C, Huang C, Zhu W, Wang X, Xu Y, Qian X (2012) A dual pH and temperature responsive polymeric fluorescent sensor and its imaging application in living cells. Chem Commun (Camb) 48 (37):4486-4488. doi:10.1039/c2cc30404j
21. Wang X-d, Meier RJ, Wolfbeis OS (2012) A Fluorophore-Doped Polymer Nanomaterial for Referenced Imaging of pH and Temperature with Sub-Micrometer Resolution. Adv Funct, Mater 22 (20):4202-4207. doi:10.1002/adfm.201200813
22. Huang H, Dong F, Tian Y (2016) Mitochondria-Targeted Ratiometric Fluorescent Nanosensor for Simultaneous Biosensing and Imaging of O2(*-) and pH in Live Cells. Anal Chem 88 (24):12294-12302. doi:10.1021/acs.analchem.6b03470
23. Moorthy MS, Cho HJ, Yu EJ, Jung YS, Ha CS (2013) A modified mesoporous silica optical nanosensor for selective monitoring of multiple analytes in water. Chem Commun (Camb) 49 (78):8758-8760. doi:10.1039/c3cc42513d
24. Yang L, Li N, Pan W, Yu Z, Tang B (2015) Real-time imaging of mitochondrial hydrogen peroxide and pH fluctuations in living cells using a fluorescent nanosensor. Anal Chem 87 (7):3678-3684. doi:10.1021/ac503975x
25. Liu J, Lu L, Li A, Tang J, Wang S, Xu S, Wang L (2015) Simultaneous detection of hydrogen peroxide and glucose in human serum with upconversion luminescence. Biosens Bioelectron 68:204-209. doi:10.1016/j.bios.2014.12.053
26. Stich MIJ, Schaeferling M, Wolfbeis OS (2009) Multicolor Fluorescent and Permeation-Selective Microbeads Enable Simultaneous Sensing of pH, Oxygen, and Temperature. Adv Mater 21 (21):2216-2220. doi:doi:10.1002/adma.200803575
27. Borisov SM, Seifner R, Klimant I (2011) A novel planar optical sensor for simultaneous monitoring of oxygen, carbon dioxide, pH and temperature. Anal Bioanal Chem 400 (8):2463-2474. doi:10.1007/s00216-010-4617-4
28. Okabe K, Inada N, Gota C, Harada Y, Funatsu T, Uchiyama S (2012) Intracellular temperature mapping with a fluorescent polymeric thermometer and fluorescence lifetime imaging microscopy. Nat Commun 3:705-709. doi:10.1038/ncomms1714
29. Kucsko G, Maurer PC, Yao NY, Kubo M, Noh HJ, Lo PK, Park H, Lukin MD (2013) Nanometre-scale thermometry in a living cell. Nature 500:54. doi:10.1038/nature12373
30. Eisele K, Gropeanu RA, Zehendner CM, Rouhanipour A, Ramanathan A, Mihov G, Koynov K, Kuhlmann CR, Vasudevan SG, Luhmann HJ, Weil T (2010) Fine-tuning DNA/albumin polyelectrolyte interactions to produce the efficient transfection agent cBSA-147. Biomaterials 31 (33):8789-8801. doi:10.1016/j.biomaterials.2010.07.088
31. Yuzhou W, Susann I, Michaela F-B, Ling KS, Klaus E, Markus L, Yanran W, Christian B, Tanja W (2013) A Core–Shell Albumin Copolymer Nanotransporter for High Capacity Loading and Two-Step Release of Doxorubicin with Enhanced Anti-Leukemia Activity. Adv Healthcare Mater 2 (6):884-894. doi:doi:10.1002/adhm.201200296
32. Amao Y, Okura I (2000) An oxygen sensing system based on the phosphorescence quenching of metalloporphyrin thin film on alumina plates. Analyst 125 (9):1601-1604. doi:10.1039/b004065g
33. Saito T, Asakura N, Kamachi T, Okura I (2007) Oxygen concentration imaging in a single living cell using phosphorescence lifetime of Pt-porphyrin. J Porphyrins Phthalocyanines 11 (03):160-164. doi:10.1142/s1088424607000205
34. Masaharu K, Norikazu T, Tomohiro H, Keisuke A, Kazuyuki N, Yutaka A (2004) Adsorptive pressure-sensitive coatings on porous anodized aluminium. Meas Sci Technol 15 (3):489
35. Nel AE, Mädler L, Velegol D, Xia T, Hoek EMV, Somasundaran P, Klaessig F, Castranova V, Thompson M (2009) Understanding biophysicochemical interactions at the nano–bio interface. Nat Mater 8:543. doi:10.1038/nmat2442

For TOC only

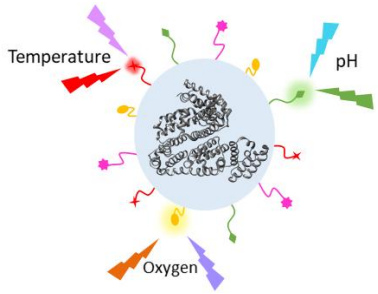

A triple nanosensor for simultaneously ratiometrically sensing intracellular pH, oxygen and temperature values were constructed by covalently labelling four fluorophores on a single serum albumin protein. The nanosensor shows good sensitivity, biocompatibility, is biodegradable and suitable for continuously measuring these important parameters.